Atmos. Meas. Tech., 15, 6387–6393, 2022
https://doi.org/10.5194/amt-15-6387-2022

Atmospheric Measurement Techniques
Open Access
EGU

Long-distance propagation of 162 MHz shipping information links associated with sporadic E

Alex T. Chartier[1], **Thomas R. Hanley**[1], **and Daniel J. Emmons**[2]

[1]Space Exploration Sector, Johns Hopkins University Applied Physics Laboratory, Laurel, MD 20723, United States of America
[2]Air Force Institute of Technology, Wright-Patterson AFB, OH 45433, United States of America

Correspondence: Alex T. Chartier (alex.chartier@jhuapl.edu)

Received: 15 July 2022 – Discussion started: 9 August 2022
Revised: 18 October 2022 – Accepted: 19 October 2022 – Published: 8 November 2022

Abstract. Sporadic E layers form in the daytime midlatitude ionosphere as a result of wind shears in the mesosphere–lower-thermosphere compressing metallic ions of meteoric origin into dense, narrow sheets extending over hundreds or thousands of kilometers spatially. These layers are poorly observed, being too narrow to be properly resolved by incoherent scatter radar or path-integrated total electron content measurements. Sporadic E layer peak densities can be resolved by ionosondes and by rocket-borne Langmuir probes, but these techniques have major limitations in terms of spatial and temporal coverage, and (for many ionosondes) maximum density resolution. As a result, the density, occurrence, and spatial extent of sporadic E layers are not well constrained by observations. The maximum density of sporadic E is widely believed to be around $5–10 \times 10^{11}$ electrons m^{-3} $N_m E_s$ (equivalent to 6–9 MHz $f_o E_s$), though there are a few isolated reports of layers extending beyond 20 MHz (Chandra and Rastogi, 1975; Maeda and Heki, 2014). Here, we identify sporadic E layers using a huge database of 29 million 162 MHz automatic identification system (AIS) shipping transmissions collected over 3 d by a United States Coast Guard (USCG) terrestrial monitoring network in the eastern United States and Puerto Rico. Within this dataset, most ($> 99\,\%$) links are explained by line-of-sight, surface-wave, and tropospheric propagation, but a small population cannot be explained by these mechanisms. In total, 6677 signals were identified from ships located over 1000 km from the ground stations between 13 and 14 July 2021, and almost no long-distance links were received at night or at any time on 15 July. This coincides with intense (saturated) sporadic E in collocated ionosondes and in satellite radio occultation data. The density of these layers might exceed 27 MHz $f_o E_s$ or 9×10^{12} electrons m^{-3} $N_m E_s$. AIS transmissions potentially provide an excellent means of identifying dense sporadic E layers globally.

1 Introduction

Automatic identification system (AIS) transponders are designed to provide vessel position, identification, and other information to other ships and to coastal authorities (e.g., International Maritime Organization, 2022). The system operates using very high-frequency (VHF) radio transmissions on two 25 kHz channels close to 162 MHz. AIS is required to be used on large ships, typically at the 12.5 W level. Many smaller vessels, including recreational boats, are also fitted with low-power (~ 2 W) or passive AIS systems. The United States Coast Guard (USCG) operates a network of land-based AIS monitors and provided 3 d of data from stations in the eastern USA and Puerto Rico for this study (13–15 July 2021) along with satellite-received data used as an independent point of reference. The exact station locations are not disclosed by request of the data provider. Occasionally, signals are identified at long distances of 1000 km or more. This long-distance propagation is surprising since signals at 162 MHz would typically be expected to pass through the ionosphere to space rather than reflecting off and back to Earth as skywaves. VHF signals do propagate over the horizon as surface waves and through tropospheric ducting (Ames et al., 1955), but the distances are typically limited to a few hundred kilometers or less. We note that very

long-distance propagation of VHF signals has been reported in amateur radio databases. For example, the "More Miles on VHF" database reports many long-distance links and attributes them to several different propagation modes, including both sporadic E and tropospheric ducting.

This study evaluates the possibility that extremely dense, low-altitude ionospheric layers (known as sporadic E) could provide a skywave propagation path that would explain the long-range USCG AIS observations. Sporadic E layers were first identified using ionosondes (e.g., Thomas and Smith, 1959). These layers are known to occur frequently, especially at midlatitudes during the daytime in summer (Wu et al., 2005; Chu et al., 2014; Arras and Wickert, 2018), with the cause believed to be a redistribution of existing plasma into thin, dense layers by wind shears (see reviews by Whitehead, 1970; Mathews, 1998; Haldoupis, 2011, for more details). The process may be aided by the presence of long-lived metallic ions deposited in the lower ionosphere by meteors (e.g., Maruyama et al., 2008). Recently, Yamazaki et al. (2022) presented convincing evidence linking sporadic E to zonal wind shears using ICON/MIGHTI interferometer wind profile data and COSMIC-2/RO retrieved electron density profiles. Deacon et al. (2022) have linked sporadic E to long-distance amateur radio propagation reports on frequencies up to 70 MHz, while amateur groups themselves routinely map sporadic E (e.g., Sampol, 2022). There are some observations of extremely high sporadic E critical frequency (f_oE_s); for example Chandra and Rastogi (1975), Maeda and Heki (2014), and Shinagawa et al. (2021) observed and modeled $f_oE_s > 20$ MHz. However the phenomenon remains unpredictable, and its occurrence, intensity, and spatial extent are not well constrained observationally, in particular over the oceans.

2 Long-distance AIS links

The USCG AIS link dataset produced by stations in the eastern USA contains almost 29 million links over 3 d. Most of the received data ($> 99\,\%$) are from ships within 300 km great-circle distance of the USCG stations. The data were processed taking care to remove any repeated signals as well as AIS signals emitted from search and rescue aircraft. A histogram of observed AIS link distances is shown in Fig. 1.

The ranges between a few hundred kilometers and $\sim$ 1000 km are likely caused by tropospheric refraction phenomena (e.g., ducting) and occur beyond the normal line of sight but are typically confined to paths within a few hundred kilometers of the coastline. As can be seen, there is a distinct population of links observed above around 1000 km great-circle distance, extending up to a maximum of 5453 km (6692 links > 1000 km in total). A time series of these links is shown in Fig. 2, with a representative day–night boundary for Bar Harbor, ME, included for reference.

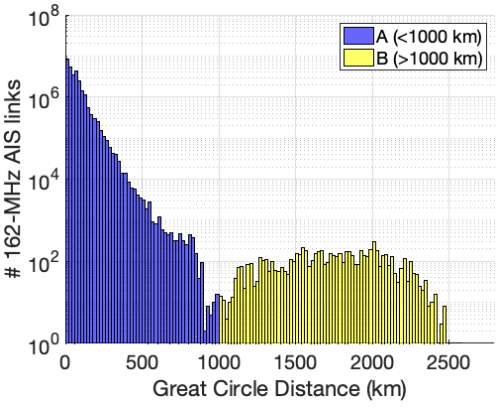

Figure 1. Histogram of AIS link great-circle distances from the USCG network in the eastern USA covering 13–15 July 2021. Population A (< 1000 km) might be explained by line-of-sight propagation, surface waves, and tropospheric ducting, while Population B (> 1000 km) is not predicted by those mechanisms. The longest reported link in our dataset covered a great-circle distance of 5453 km (not shown).

Almost all (6677) of the long-distance AIS links were detected on 13 and 14 July, with almost none seen at night or on 15 July. The maximum number of long-range links in a 15 min window was 655, between 18:45–19:00 UT on 14 July, and the second highest number was 421, between 14:15–14:30 UT on 13 July. Snapshots of these intervals are shown in Fig. 3.

These snapshots indicate the long-distance AIS propagation is related to a spatially confined phenomenon, intermittently present over an area of hundreds or thousands of kilometers during daytime hours.

3 Data identifying tropospheric ducting

Tropospheric ducting is estimated using meteorological reanalysis temperature, pressure, and humidity data. Here we computed ducting using the European Centre for Medium-Range Weather Forecasts (ECMWF) 5th Generation Reanalysis (ERA5) described by Hersbach et al. (2018). These data were processed to compute the maximum strength of all radio frequency (RF)/tropospheric ducts that appear at a single grid point and time. The maps of modified refractivity were derived from hourly forecast data using the full-resolution 137 level temperature and specific humidity data provided on a regular Gaussian grid, at hourly resolution. Ducting maps at 19:00 UT on 14 July and 14:00 UT on 13 July are shown in Fig. 4.

By showing the tropospheric ducting strength overlaid with the received position reports from land-based AIS receivers, one can see the correlations near shore of the tropospheric ducting that helps to extend the RF propagation range. It is also apparent that tropospheric ducting could not

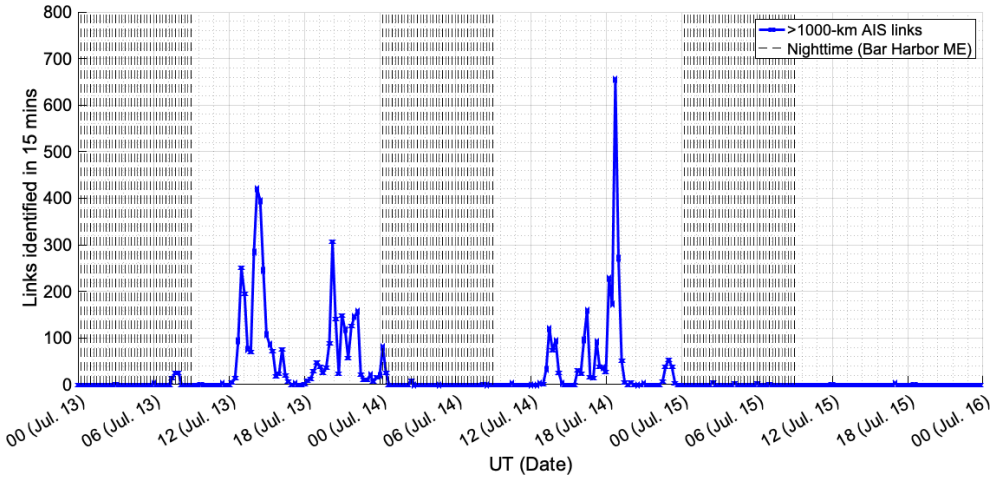

Figure 2. Figure 2 shows AIS links received from ships at over 1000 km great-circle distance from USCG stations between 13–15 July 2021. The results are binned in 15 min increments. Nighttime at Bar Harbor, ME, is indicated by black dashes.

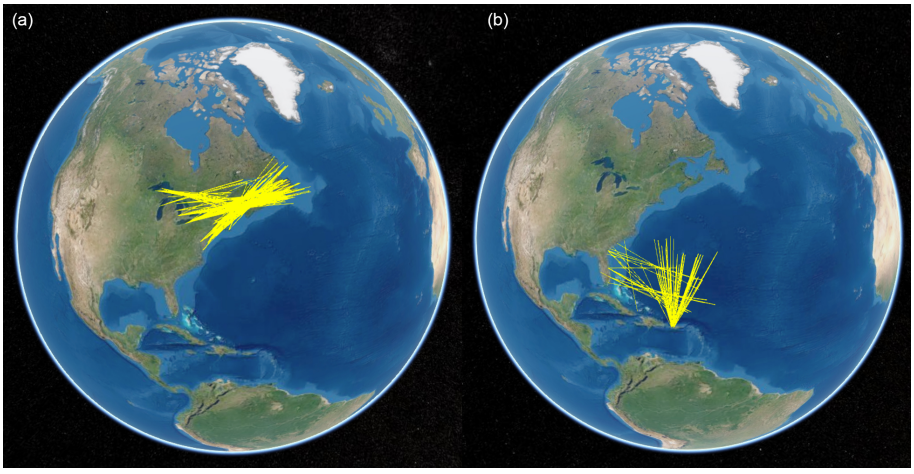

Figure 3. Figure 3 shows the long-distance AIS links identified by USCG stations **(a)** between 18:45–19:00 UT on 14 July 2021 and **(b)** between 14:15–14:30 UT on 13 July 2021.

be responsible for the very long-range AIS receptions that are the main focus of this publication. To illustrate this, a time series of the median nonzero tropospheric duct strength is shown in Fig. 5.

As can be seen in Fig. 5, tropospheric ducting peaks on 15 July 2021, when almost no long-distance AIS links were observed. Therefore a different explanation is needed for the $>$ 1000 km propagation observed on 162 MHz that were shown in Fig. 2.

4 Data identifying sporadic E

Data from ground-based Digisondes and from Constellation Observing System for Meteorology, Ionosphere, and Climate (COSMIC-2) radio occultations are used to identify the cause of the observed long-distance AIS links. Figure 6 shows Digisonde peak sporadic E plasma frequency (f_oE_s) from Millstone Hill, MA; Wallops Island, VA; and Ramey, Puerto Rico.

The Digisonde f_oE_s values saturate (i.e., they reach the maximum observable value of 10 MHz at Millstone and Wallops or 6.5 MHz at Ramey) during the daytime at Wallops and Ramey on 13 July and at Wallops and Millstone on 14 July. The data do not saturate at any station either at night or at any time on 15 July. This is consistent with the trend seen in the long-distance AIS link data.

Spatial maps of sporadic E are produced by combining COSMIC-2 RO data with Digisonde measurements, using the S_4-based approach described by Yu et al. (2020). These maps are produced at 3 h cadence to increase the number of local observations in the region. Maps corresponding to the two maximum AIS link times are shown in Fig. 7.

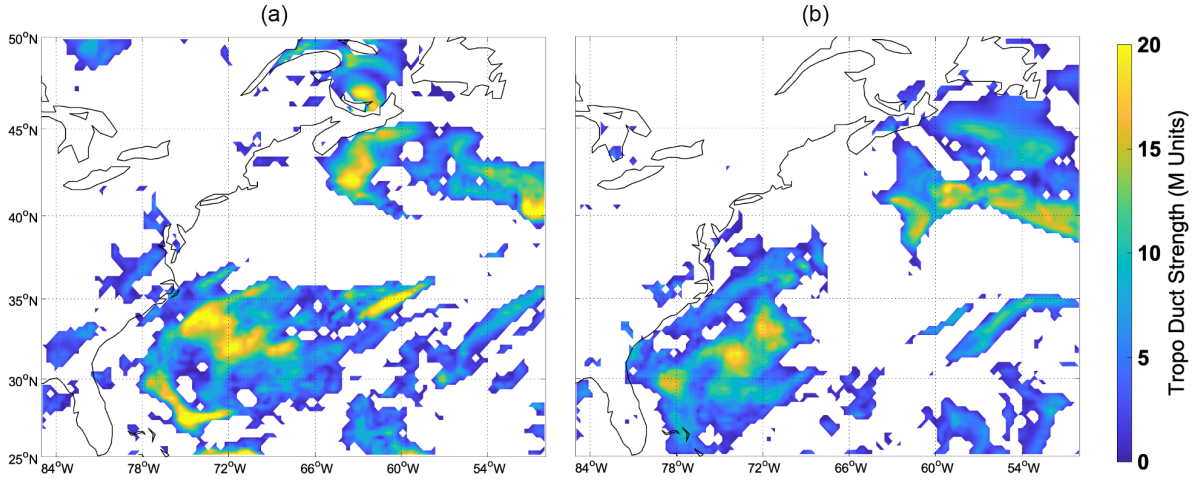

Figure 4. Figure 4 shows tropospheric ducting maps of modified refractivity (in M units) based on temperatures, pressures, and humidities in ERA5 reanalysis data. Panel **(a)** shows 19:00 UT on 14 July 2021, while panel **(b)** shows 14:00 UT on 13 July 2021.

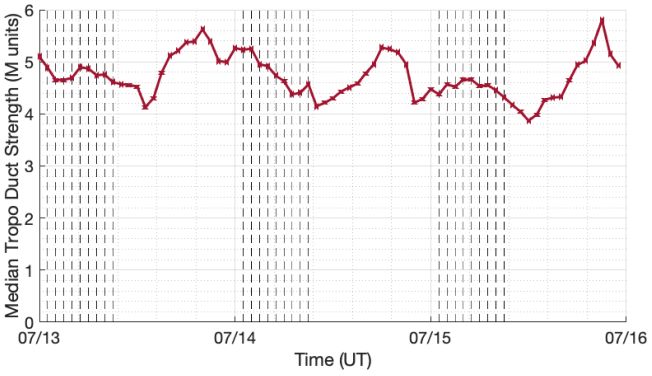

Figure 5. Median nonzero tropospheric duct strength between 25–50° N and 85–50° E between 13–15 July 2021. Nighttime at Bar Harbor, ME, is shown by black dashed lines.

Given the spatial and temporal limitations of the data coverage, the sporadic E maps show remarkably good agreement with the AIS long-distance link data shown in Fig. 3. While the COSMIC-2 RO data are useful in identifying the presence or absence of sporadic E (Carmona et al., 2022), predicting f_oE_s magnitudes from RO data is more difficult (Gooch et al., 2020). This is especially true of strong sporadic E layers that tend to saturate the S_4 amplitude scintillation (Stambovsky et al., 2021; Yu et al., 2020). Therefore, we have higher confidence in the f_oE_s estimates near Digisondes than in the locations driven strictly by RO data.

5 Discussion and conclusions

The analysis indicates that long-distance 162 MHz AIS links observed in the western Atlantic region on 13 and 14 July 2021 are associated with sporadic E layers. This is remarkable given that signals at such high frequency are typically expected to pass through the ionosphere. The available vertical-incidence ionosonde data in the region saturate at or below 10 MHz, so it is not possible to determine the true value of f_oE_s during these periods.

If we assume a layer height of 100 km and take the shortest AIS paths within the anomalous distribution at around 1200 km (see Fig. 1), we can estimate an angle of incidence $\sim 9.5°$ (neglecting refraction and curvature). In this case the secant law (see Han, 1970, for details) implies $f_oE_s >= 27$ MHz or 9×10^{12} electrons m^{-3}. This is almost an order of magnitude larger than is typically expected, though there have been observations of $f_oE_s > 20$ MHz (Chandra and Rastogi, 1975; Maeda and Heki, 2014).

There are several challenges inherent in using AIS data to identify long-distance propagation. In some cases the system is subject to spoofing, either of the signals themselves or the GNSS signals they rely upon. There are also occasional transmission errors that still pass the checksum. Therefore accurate determination of long-distance propagation requires the identification of multiple unique vessels over similar geometries. To avoid random errors, it is useful to observe multiple reports from a given ship over a few minutes; to observe consistency between the reported position, time, speed, and course; and to cross-reference with other information, such as ports of call. We have applied these techniques in filtering the AIS data, but the removal of erroneous data remains an open challenge.

In summary, long-distance AIS links appear to be a promising means of observing dense sporadic E layers. The data have several advantages, notably high power, high density of users and high cadence due to internationally mandated usage, and coverage over the oceans. The USCG dataset used here is not routinely available, but the protocol is public and transponders are widespread on ships and ground stations. Therefore much of the infrastructure is al-

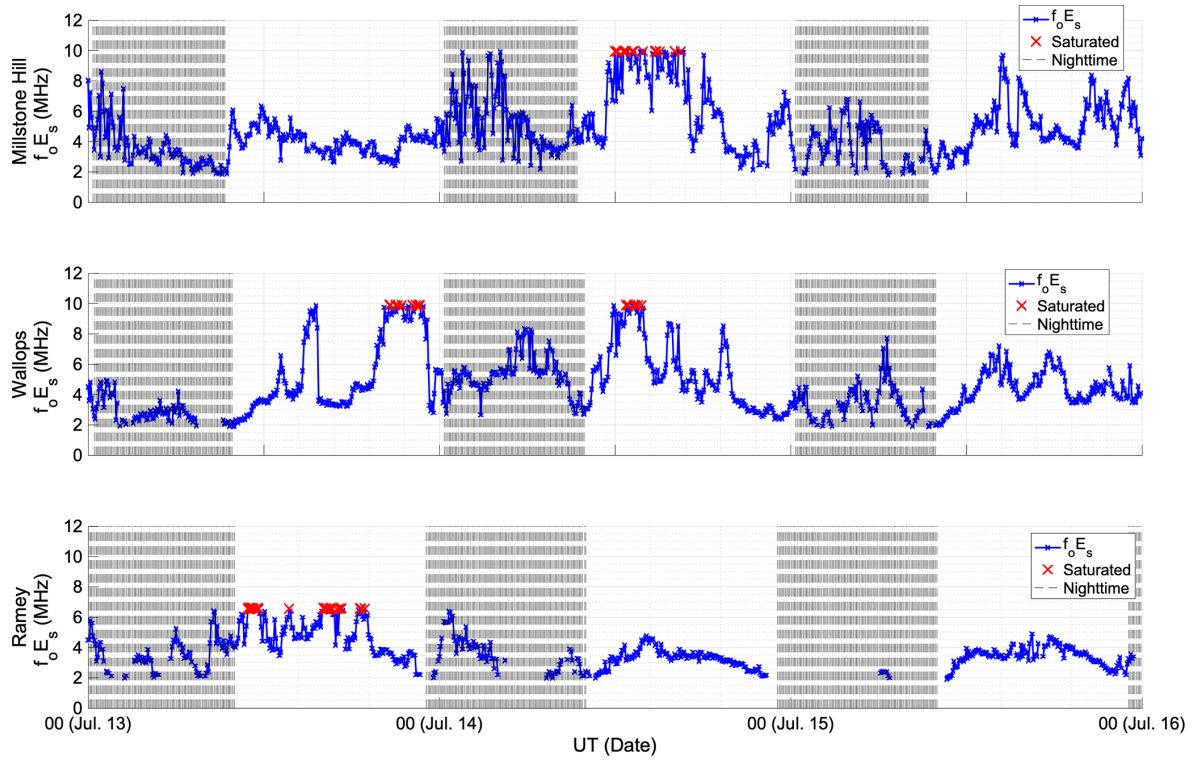

Figure 6. Autoscaled sporadic E data from the Millstone Hill, Wallops, and Ramey Digisondes. Saturated measurements where f_oE_s exceeded the ionosonde's frequency range are shown in red. Local nighttime is indicated by black dashed lines.

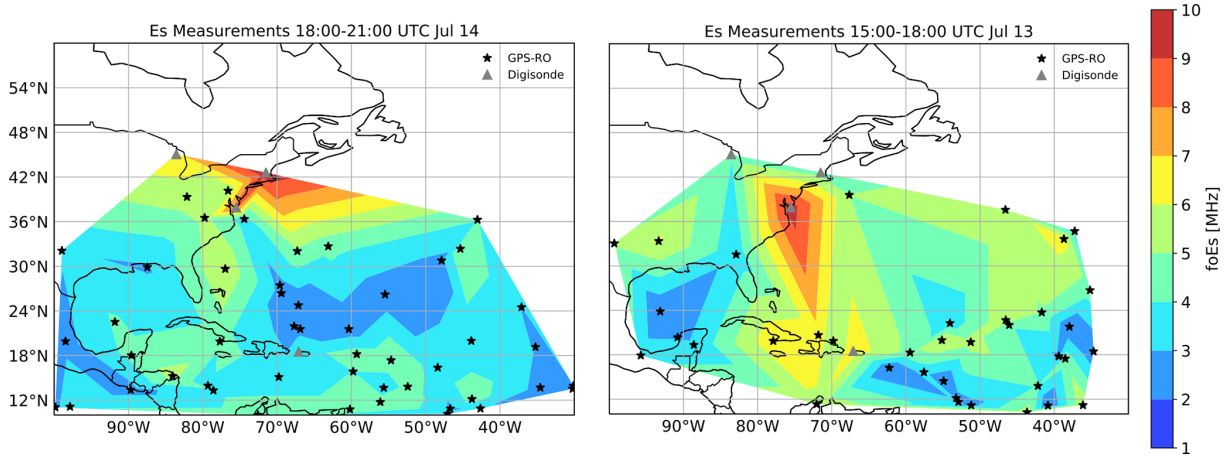

Figure 7. Figure 7 shows sporadic E maps based on Digisonde and COSMIC-2 RO S4 data for 18:00–21:00 UT on 14 July 2021 and 15:00–18:00 UT on 13 July 2021.

ready in place to develop a worldwide monitoring network. This study indicates skywave propagation due to sporadic E layers is possible at higher frequencies than we were able to find previously reported in the literature, though we have not performed an exhaustive search.

Code availability. Data analysis code is available here: https://doi.org/10.5281/zenodo.7278089 (Chartier, 2022b).

Data availability. Digisonde data can be retrieved from http://giro.uml.edu/didbase/scaled.php (Global Ionosphere Radio Observatory, 2022). COSMIC-2 data are available from https://doi.org/10.5065/t353-c093 (UCAR COSMIC Program, 2019), while the sporadic E maps for our study are available at

https://doi.org/10.5281/zenodo.6977022 (Emmons, 2022). Tropospheric ducting files are at https://doi.org/10.5281/zenodo.7140002 (Hanley and Chartier, 2022). The AIS data used here are not accessible to the public or research community, but it may be possible to obtain them from USCG by request. We note that public repositories of other VHF radio link data exist that may be useful for independent validation of these findings (e.g. https://www.wsprnet.org/drupal/, last access: 3 November 2022; https://pskreporter.info/pskmap.html, last access: 3 November 2022; https://mmmonvhf.de/odx.php, last access: 3 November 2022).

Video supplement. The full set of our > 1000 km AIS links can be viewed at https://www.youtube.com/watch?v=AcNzM03zZP8 (Chartier, 2022a).

Author contributions. ATC wrote the paper, produced Figs. 1–6, and submitted the paper. TRH performed the AIS data analysis and first raised the possibility that these long-distance links were related to ionospheric phenomena. DJE performed the ionosonde–GNSS sporadic E analysis and produced Fig. 7.

Competing interests. The contact author has declared that none of the authors has any competing interests.

Disclaimer. Publisher's note: Copernicus Publications remains neutral with regard to jurisdictional claims in published maps and institutional affiliations.

Acknowledgements. Alex T. Chartier acknowledges support of NASA (grant no. 80NSSC21K1557).

Financial support. This research has been supported by the National Aeronautics and Space Administration (grant no. 80NSSC21K1557)

Review statement. This paper was edited by Jorge Luis Chau and reviewed by two anonymous referees.

References

Ames, L. A., Newman, P., and Rogers, T. F.: VHF tropospheric overwater measurements far beyond the radio horizon, Proceedings of the IRE, 43, 1369–1373, 1955.

Arras, C. and Wickert, J.: Estimation of ionospheric sporadic E intensities from GPS radio occultation measurements, J. Atmos. Sol.-Terr. Phy., 171, 60–63, 2018.

Carmona, R. A., Nava, O. A., Dao, E. V., and Emmons, D. J.: A Comparison of Sporadic-E Occurrence Rates Using GPS Radio Occultation and Ionosonde Measurements, Remote Sens., 14, 581, https://doi.org/10.3390/rs14030581, 2022.

Chandra, H. and Rastogi, R. G.: Blanketing sporadic E layer near the magnetic equator, J. Geophys. Res., 80, 149–153, 1975.

Chartier, A.: Long distance AIS links associated with sporadic-E, YouTube [video], https://www.youtube.com/watch?v=AcNzM03zZP8, last access: 3 November 2022a.

Chartier, A. T.: AMT sporadic E paper code release, Zenodo [code], https://doi.org/10.5281/zenodo.7278089, 2022b.

Chu, Y. H., Wang, C. Y., Wu, K. H., Chen, K. T., Tzeng, K. J., Su, C. L., and Plane, J. M. C.: Morphology of sporadic E layer retrieved from COSMIC GPS radio occultation measurements: Wind shear theory examination. J. Geophys. Res.-Space Phys., 119, 2117–2136, 2014.

Deacon, C., Mitchell, C., and Watson, R.: Consolidated Amateur Radio Signal Reports as Indicators of Intense Sporadic E Layers, Atmosphere, 13, 906, https://doi.org/10.3390/atmos13060906, 2022.

Emmons, D.: GNSS and Digisonde sporadic-E maps produced by Air Force Institute of Technology, Zenodo [data set], https://doi.org/10.5281/zenodo.6977022, 2022.

Global Ionosphere Radio Observatory: FastChar – Digital Ionogram Data Base (DIDBase), GIRO [data set], http://giro.uml.edu/didbase/scaled.php, last access: 3 November 2022.

Gooch, J. Y., Colman, J. J., Nava, O. A., and Emmons, D. J.: Global ionosonde and GPS radio occultation sporadic-E intensity and height comparison, J. Atmos. Sol.-Terr. Phy., 199, 105200, https://doi.org/10.1016/j.jastp.2020.105200, 2020.

Haldoupis, C.: A tutorial review on sporadic *E* layers, Aeronomy of the Earth's Atmosphere and Ionosphere, 381–394, https://doi.org/10.1007/978-94-007-0326-1_29, 2011.

Han, R.-Y.: A Study of The Secant Law for Sporadic E, All Graduate Theses and Dissertations, 3322, https://digitalcommons.usu.edu/etd/3322 (last access: 3 November 2022), 1970.

Hanley, T. R. and Chartier, A. T.: Tropospheric ducting maps, Zenodo [data set], https://doi.org/10.5281/zenodo.7140002, 2022.

Hersbach, H., Bell, B., Berrisford, P., Biavati, G., Horányi, A., Muñoz Sabater, J., Nicolas, J., Peubey, C., Radu, R., Rozum, I., Schepers, D., Simmons, A., Soci, C., Dee, D., and Thépaut, J-N.: ERA5 hourly data on pressure levels from 1959 to present, Copernicus Climate Change Service (C3S) Climate Data Store (CDS), https://doi.org/10.24381/cds.bd0915c6, 2018.

International Maritime Organization: AIS Transponders, https://www.imo.org/en/OurWork/Safety/Pages/AIS.aspx, last access: 1 June 2022.

Maeda, J. and Heki, K.: Two-dimensional observations of midlatitude sporadic E irregularities with a dense GPS array in Japan, Radio Sci., 49, 28–35, 2014.

Maruyama, T., Kato, H., and Nakamura, M.: Meteor-induced transient sporadic E as inferred from rapid-run ionosonde observations at midlatitudes, J. Geophys. Res.-Space Phys., 113, A9, https://doi.org/10.1029/2008JA013362, 2008.

Mathews, J. D.: Sporadic E: current views and recent progress, J. Atmos. Sol.-Terr. Phy., 60, 413–435, 1998.

Sampol, G.: 144 MHz Sporadic-E QSO maps. Years 2003 to 2021, https://www.dxmaps.com/esmaps/oldesmaps.html, last access: 10 June 2022.

Shinagawa, H., Tao, C., Jin, H., Miyoshi, Y., and Fujiwara, H.: Numerical prediction of sporadic E layer occurrence using GAIA, Earth Planets Space, 73, 1–18, 2021.

Stambovsky, D. W., Colman, J. J., Nava, O. A., and Emmons, D. J.: Simulation of GPS radio occultation signals through Sporadic-E using the multiple phase screen method., J. Atmos. Sol.-Terr. Phy., 214, 105538, https://doi.org/10.1016/j.jastp.2021.105538, 2021.

Thomas, J. A. and Smith, E. K.: A survey of the present knowledge of sporadic-E ionization, J. Atmos. Sol.-Terr. Phy., 13, 295–314, 1959.

UCAR COSMIC Program: COSMIC-2 Data Products, UCAR [data set], https://doi.org/10.5065/t353-c093, 2019.

Whitehead, J. D.: Production and prediction of sporadic E, Rev. Geophys., 8, 65–144, 1970.

Wu, D. L., Ao, C. O., Hajj, G. A., de La Torre Juarez, M., and Mannucci, A. J.: Sporadic *E* morphology from GPS-CHAMP radio occultation, J. Geophys. Res.-Space Phys., 110, A01306, https://doi.org/10.1029/2004JA010701, 2005.

Yamazaki, Y., Arras, C., Andoh, S., Miyoshi, Y., Shinagawa, H., Harding, B. J., Englert, C. R., Immel, T. J., Sobhkhiz-Miandehi, S., and Stolle, C.: Examining the Wind Shear Theory of Sporadic E with ICON/MIGHTI Winds and COSMIC-2 Radio Occultation Data, Geophys. Res. Lett., 49, e2021GL096202, https://doi.org/10.1029/2021GL096202, 2022.

Yu, B., Scott, C. J., Xue, X., Yue, X., and Dou, X.: Derivation of global ionospheric Sporadic E critical frequency (fo Es) data from the amplitude variations in GPS/GNSS radio occultations, Roy. Soc. Open Sci., 7, 200320, https://doi.org/10.1098/rsos.200320, 2020.